MML TR-80-17-c

BONDABILITY OF TI ADHERENDS

Martin Marietta Laboratories
1450 South Rolling Road
Baltimore, Maryland 21227

30 April 1980

Final Report 4/1/79 - 3/31/80

Prepared for

Naval Air Systems Command
Code AIR-52032-B
Washington, D.C. 20361

Baltimore DCAS Management Area
300 E. Joppa Road, Room 200
Towson, Maryland 21204
Attention: Mr. William L. Sunday, ACO

SECURITY CLASSIFICATION OF THIS PAGE (When Data Entered)

REPORT DOCUMENTATION PAGE		READ INSTRUCTIONS BEFORE COMPLETING FORM
1. REPORT NUMBER	2. GOVT ACCESSION NO. AD-A094624	3. RECIPIENT'S CATALOG NUMBER
4. TITLE (and Subtitle) "Bondability of Ti Adherends"		5. TYPE OF REPORT & PERIOD COVERED Final Report (1st year) 4/1/79 - 3/31/80
		6. PERFORMING ORG. REPORT NUMBER MML TR-80-17c
7. AUTHOR(s) B. M. Ditchek, K. R. Breen, J. D. Venables		8. CONTRACT OR GRANT NUMBER(s) N00019-79-C-0294
9. PERFORMING ORGANIZATION NAME AND ADDRESS Martin Marietta Laboratories, 1450 South Rolling Road, Baltimore, Md. 21227		10. PROGRAM ELEMENT, PROJECT, TASK AREA & WORK UNIT NUMBERS
11. CONTROLLING OFFICE NAME AND ADDRESS Naval Air Systems Command, Code AIR-52032-B, Washington, D.C. 20361		12. REPORT DATE April 30, 1980
		13. NUMBER OF PAGES 51
14. MONITORING AGENCY NAME & ADDRESS(if different from Controlling Office) Baltimore DCAS Management Area, 300 E. Joppa Road, Room 200, Towson, Maryland 21204, Attention: Mr. William L. Sunday, ACO		15. SECURITY CLASS. (of this report) Unclassified
		15a. DECLASSIFICATION/DOWNGRADING SCHEDULE

16. DISTRIBUTION STATEMENT (of this Report)
Approved for public release; distribution unlimited

17. DISTRIBUTION STATEMENT (of the abstract entered in Block 20, if different from Report)
N.A.

18. SUPPLEMENTARY NOTES

19. KEY WORDS (Continue on reverse side if necessary and identify by block number)
titanium, bonding, adhesion, bondability, oxide morphology, adherends, surface treatment, durability

20. ABSTRACT (Continue on reverse side if necessary and identify by block number)

Surface oxides on titanium prepared for adhesive bonding by eight different pretreatment processes were examined using STEM and Auger/ESCA techniques. The results indicate that the surfaces can be divided into three groups according to similarities in their oxide morphologies: Group I exhibits little surface roughness; Group II is characterized by macro-roughness (features >1.0 μm); and Group III exhibits extensive porosity and micro-roughness, similar to features found on aluminum prepared by the phosphoric

DD FORM 1 JAN 73 1473

SECURITY CLASSIFICATION OF THIS PAGE (When Data Entered)

Block 20. ABSTRACT (Continued)

acid anodize process. Wedge tests (performed at NADC, but discussed here) indicate that Group III adherends (chromic acid anodize and alkaline peroxide treatments) produce far more durable bonds than those in Groups I or II. Hence, a direct correlation exists between oxide morphology and bond durability for Ti adherends.

We found similar evidence of the importance of oxide morphology to the properties of bondments in our prior work on Al but with one important difference. Because Al oxides are relatively unstable in a moist environment, the bond can suffer long-term degradation. In contrast, the Ti oxides are extremely stable against the effects of moisture. We conclude, therefore, that the combination of oxide stability and micro-roughness that can be developed on Ti by the CAA or alkaline peroxide processes portends a very bright future for adhesively bonded Ti structures.

TABLE OF CONTENTS

LIST OF FIGURES

LIST OF FIGURES (continued)

LIST OF FIGURES (continued)

1. INTRODUCTION

Although many factors can affect the durability and integrity of adhesively bonded metal structures, it has been realized for years that proper chemical treatment of the metal prior to adhesive bonding is essential for developing the bond strengths necessary for high-performance aircraft applications. In the past, surface preparation methods have been developed principally through an empirical approach, often with little understanding of why one method was superior (or inferior) to another. More recently, however, various investigators have suggested that the microscopic morphology of the surface oxide which is formed in the pretreatment process is important in determining the bondability of the metal parts.[1-6] In particular, recent work at Martin Marietta Laboratories, using ultra-high resolution scanning transmission electron microscopy (STEM), has demonstrated conclusively that two commercially important pretreatment processes for Al adherends are successful because they provide favorable oxide morphologies, i.e., those that can interlock mechanically with the adhesive to form a much stronger bond than would be otherwise possible.[6]

The STEM, operated in the SEM mode, has an order-of-magnitude greater resolving power than a conventional SEM (20 Å vs 200 Å). Consequently,

1. P.F.A. Bijlmer, J. Adhesion 5, 319 (1975).
2. P.F.A. Bijlmer and R.J. Schliekelman, SAMPE Quarterly 5(1), 13 (1973).
3. A. Pattnaik and J.D. Meakin, Franklin Institute Research Laboratories Technical Report 4699, 1974.
4. T. Smith, Rockwell International Report AFML-TR-74-73, 1975.
5. J.M. Chen, T.S. Sun, J.D. Venables, and R. Hopping, Proc. 22nd National SAMPE Symposium (San Diego, CA, 1977) p. 25.
6. J.D. Venables, D.K. McNamara, J.M. Chen, T.S. Sun, and R.L. Hopping, Appl. Surface Sci. 3, 88 (1979).

this technique is ideally suited for studying the morphology of oxides on Al. For example, using this instrument, we (at Martin Marietta Laboratories) were the first to observe 100 Å-diameter oxide whiskers protruding from the surface of the oxide. These whiskers provide a "fiber reinforced interface" between the oxide and epoxy, thus increasing the bond strength.[5,6]

In addition to using the STEM to observe the morphology of Al adherends, researchers at Martin Marietta Laboratories have also used Auger/ESCA techniques to characterize the chemical nature of these surfaces, and electron diffraction to determine the atomic arrangement in the oxides. Using similar techniques, we have attempted to characterize Ti adherends prepared according to a variety of different pretreatment processes. Unlike the adhesive bonding of Al, in which only three main pretreatment processes (FPL, PAA, or CAA) are used, Ti bonding involves many more processes.

Historically, the poor durability of adhesively bonded titanium prepared by alkaline cleaning as well as the phosphate fluoride process was first pointed out by Wegman.[7] He subsequently developed a modified phosphate fluoride process that increased time-to-failure of stressed lap shear panels by nearly an order of magnitude. The durability of bonds to these surfaces has been compared with that produced by other chemical pretreatments, such as the Turco 5578 and the VAST abrasive surface treatment, by Felsen.[8] (However, Felsen found, in contrast with Wegman's results, that the surface pretreatments produced very similar bond durability.)

7. R.F. Wegman and M.J. Bondnar, SAMPE Quarterly 5, 28 (1973).
8. M.J. Felsen, "Materials Synergisms," Proc. 10th National SAMPE Technical Conference Series, Vol. 10, p. 100, 1978.

In another comparative study, alkaline peroxide treatments were found to yield more durable bonds than the modified and original phosphate fluoride processes.(9) Other processes combine abrasive and chemical treatments, such as liquid hone PASA JELL 107 treatment, which abrades with a slurry of alumina particles, and dry hone PASA JELL 107 treatment, which abrades dry. In addition, an anodization process has been developed that uses chromic acid doped with ammonium fluoride.(10)

To determine the surface morphology and surface chemistry produced by these pretreatments, and which provides the most durable bonds, a program was developed to evaluate these pretreatments in three coordinated tasks:

1) Studies of both prebonded and adhesively failed surfaces using the STEM in both the high-resolution SEM and electron diffraction modes, and Auger/ESCA techniques.
2) Lap shear tests of bonded and primed Ti-6Al-4V panels.
3) Wedge tests of bonded and primed Ti-6Al-4V panels.

In this program, we at the Laboratories are performing the surface analysis while Wegman at AARADCOM and Brown at NADC are performing the lap shear and wedge tests, respectively. In this report, we present the results of our studies on the bondability of Ti adherends.

---

9. A. Mahoon and J. Cotter, ibid., p. 425.
10. Y. Maji and J.A. Marceau, U.S. Patent 3,959,091, May 25, 1976.

2. EXPERIMENTAL PROCEDURE

Surface Treatment

Table 1 lists all the pretreatments used to prepare Ti adherends (the Ti symbol is used throughout to indicate the Ti-6Al-4V alloy). Except for the alkaline peroxide-treated specimens, all surfaces were prepared elsewhere.

Mechanical Testing

Wedge and lap shear tests were performed by Brown and Wegman, respectively. The failure analysis reported here was performed on specimens that they supplied to us.

Sample Preparation

Specimen surfaces were examined by SEM in a JEOL 100-CX STEM. To reduce charging, the surfaces were coated with an extremely thin layer of Pt using secondary ion deposition. Only the minimum coating thickness (~ 20 Å) needed for charge suppression was applied to avoid obscuring surface fine structure. Stereo pairs of the surface were obtained on a split screen CRT using a 7° tilt angle.

Since adhesive bonding directly involves only the top few atomic layers of the oxide, a contaminant only a fraction of a monolayer thick could reduce the bond strength significantly. To analyze the chemical composition of the pretreatment surface, both ESCA and AES were used. An Ar+ ion sputtering gun incorporated in the electron spectrometer (Physical Electronics/model 548) enabled us to obtain depth profiles of the monitored

TABLE 1

MORPHOLOGICAL CHARACTERISTICS AND CHEMICAL CONTAMINANTS ASSOCIATED WITH VARIOUS TI PRETREATMENT PROCESSES

Process	Process Code	Oxide Thickness (Å)	Group[a] Number	*Comments*
1. Phosphate fluoride	PF	200	I	F contamination
2. Modified phosphate fluoride	MPF	80	I	F contamination
3. Dapcotreat	DA	60	II	No apparent fine structure; Cr on surface
4. Dry hone PASA JELL 107	DP	100–200	II	Deformed surface with embedded Al_2O_3; fluorine contamination
5. Liquid hone PASA JELL 107	LP	200	II	Embedded alumina; fluorine contaminant; Cr on surface
6. Turco 5578	TU	175	II	Fe containing particles on surface
7. Chromic acid anodize	CAA	5V:400 10V:800	III	Porous oxide with protruding whiskers; flourine contamination
8. Alkaline peroxide	AP	450–1350 depending on chemistry, temperature, time	III	Porous oxide

[a] For a definition of group numbers, see text.

species. Auger depth profiles were also used to estimate oxide thickness. Sun et al. have presented[11] a discussion on Auger depth profiling of adherends to determine oxide thicknesses.

Crystal structure analysis of the adherends produced by the various pretreatments was performed using the electron diffraction mode of the TEM portion of the STEM. Thin films suitable for electron transmission were prepared by ion milling. Oxides were then grown on these thin metallic films by using the various pretreatments.

11. T.S. Sun, D.K. McNamara, J.S. Ahearn, B.M. Ditchek, J.D. Venables, and J.M. Chen, submitted to Applications of Surface Science.

3. RESULTS

Characterization of Ti Adherends

Table 1 lists the various surface treatments investigated in this study and provides some comments on their effect on Ti surfaces. Although the appearances of these treated surfaces varied considerably, it was possible to categorize them into three groups according to similarities in their morphologies. Group I adherends, which include both the PF and MPF pretreatments (notation defined in Table 1), display little macro- or micro-roughness.* Group II adherends, on the other hand, all exhibit a large degree of macro-roughness. The DA, LP, TU, and DP pretreatments are all in this set. Group III adherends include surfaces treated by either chromic acid anodization or an alkaline peroxide etch. They are characterized by a porous oxide with high micro-roughness and low macro-roughness. The details of the characteristics of Ti surfaces treated according to Group I, II, and III pretreatments are discussed below.

Group I Pretreatments -- Viewed at low magnification (~ 1000X), the PF- and MPF-treated adherends appear similar. The surface contrast is generated primarily by a difference in the etching rate of the α(hcp) and β(bcc) phases: the β phase, which is etched more slowly then the α phase, appears in high relief at the surface. Low-magnification images of these two adherends appear similar to those presented in conventional SEM or replica

* A macro-rough surface is defined as an uneven surface with characteristic bumps or jagged edges about 1.0 μm or greater. Micro-rough surfaces have fine structures with dimensions of 0.1 μm or less.

TEM micrographs obtained by other investigators.[4,12] An example of a PF surface is shown in Figure 1.

At higher magnifications (20,000X and up), a fine surface morphology can be detected that distinguishes the two processes in this group. Figures 2a and 2b show stereo micrographs of the fine structure on PF- and MPF-treated surfaces, respectively. The fine structure shown in Figure 2a is distributed evenly through the α phase, while the ridges formed by the MPF process, shown in Figure 2b, vary in height and degree of coverage from one grain to another. In both cases, the β-phase oxide is relatively smooth and featureless. In general, neither of these adherends exhibits sufficient roughness to yield a significant mechanical component in bond strength.

The thickness of the PF oxide was found to be 200 Å, based on the time required to remove it by sputtering. This value agrees with Smith's ellipsometric measurement.[4] However, the MPF oxide was only about 80 Å thick.

Auger analysis of these adherend surfaces suggested that small quantities of the pretreatment chemicals used in the PF process adsorbed onto the surface. For example, the spectra from the MPF-treated adherend (Figure 3) indicate that Na (from the Na_3PO_4) and F (from HF and KF) are retained on the surface.

Electron diffraction from thin films treated according to the PF specifications yielded little detectable contribution from the thin (less than 100 Å) oxide. The diffuse scattering observed was too weak to be accurately indexed.

---

12. K.W. Allen and H.S. Abalin, J. Adhesion 6, 229 (1974).

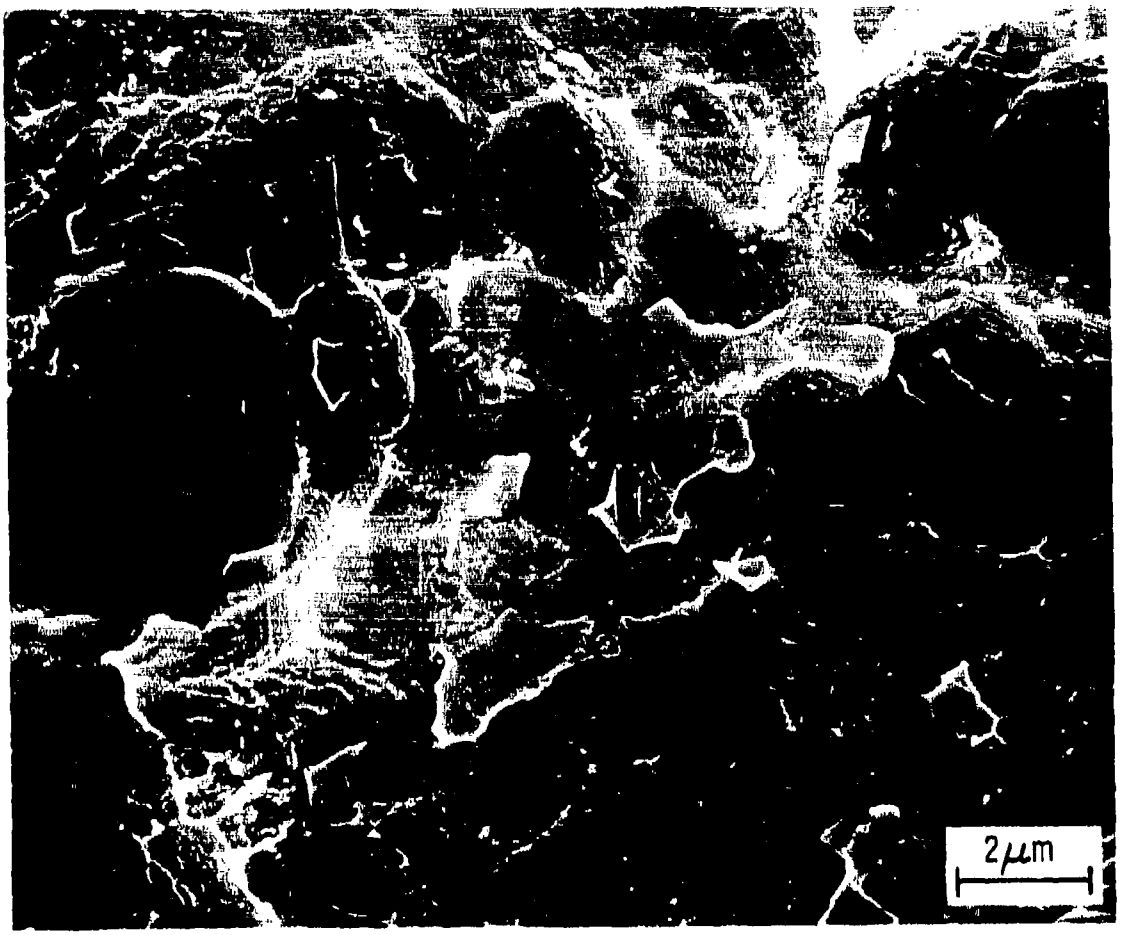

Figure 1. A collage of electron micrographs of the surface of PF-treated Ti. This adherend shows little macro-roughness.

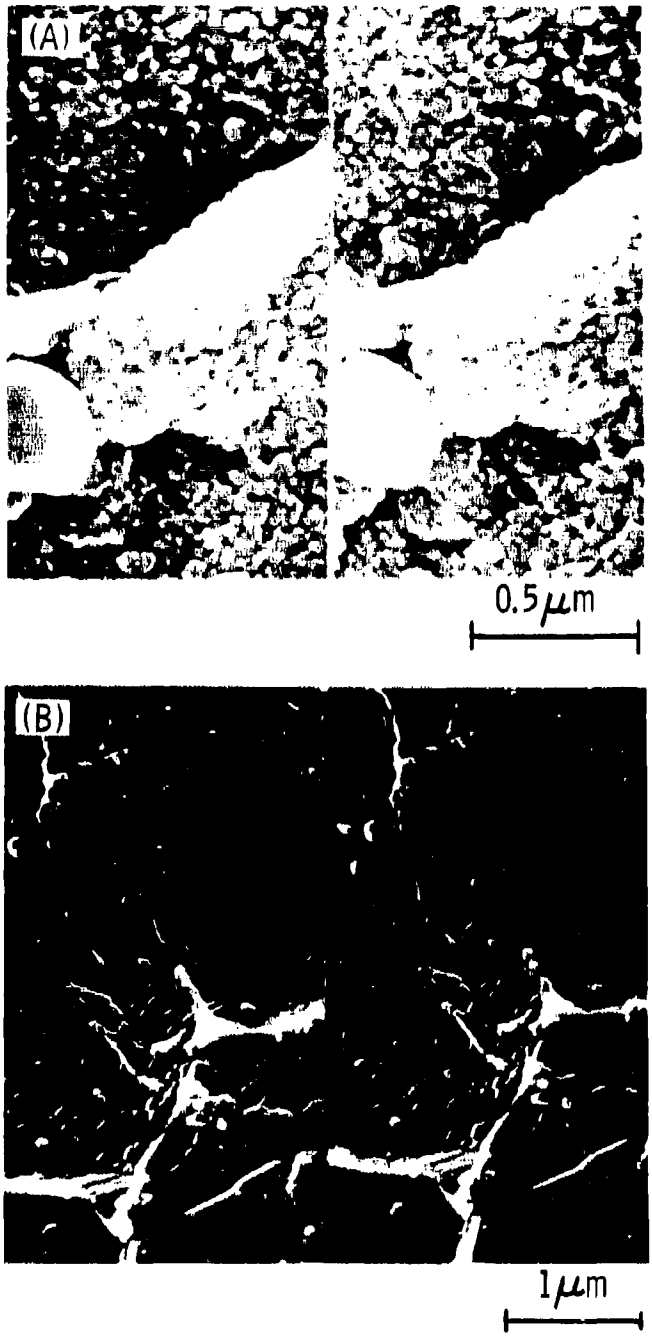

Figure 2. Stereo electron micrographs of Ti adherends treated by (A) phosphate fluoride process and (B) modified phosphate fluoride process. Neither of these adherends provides sufficient micro-roughness to promote mechanical interlocking with the primer.

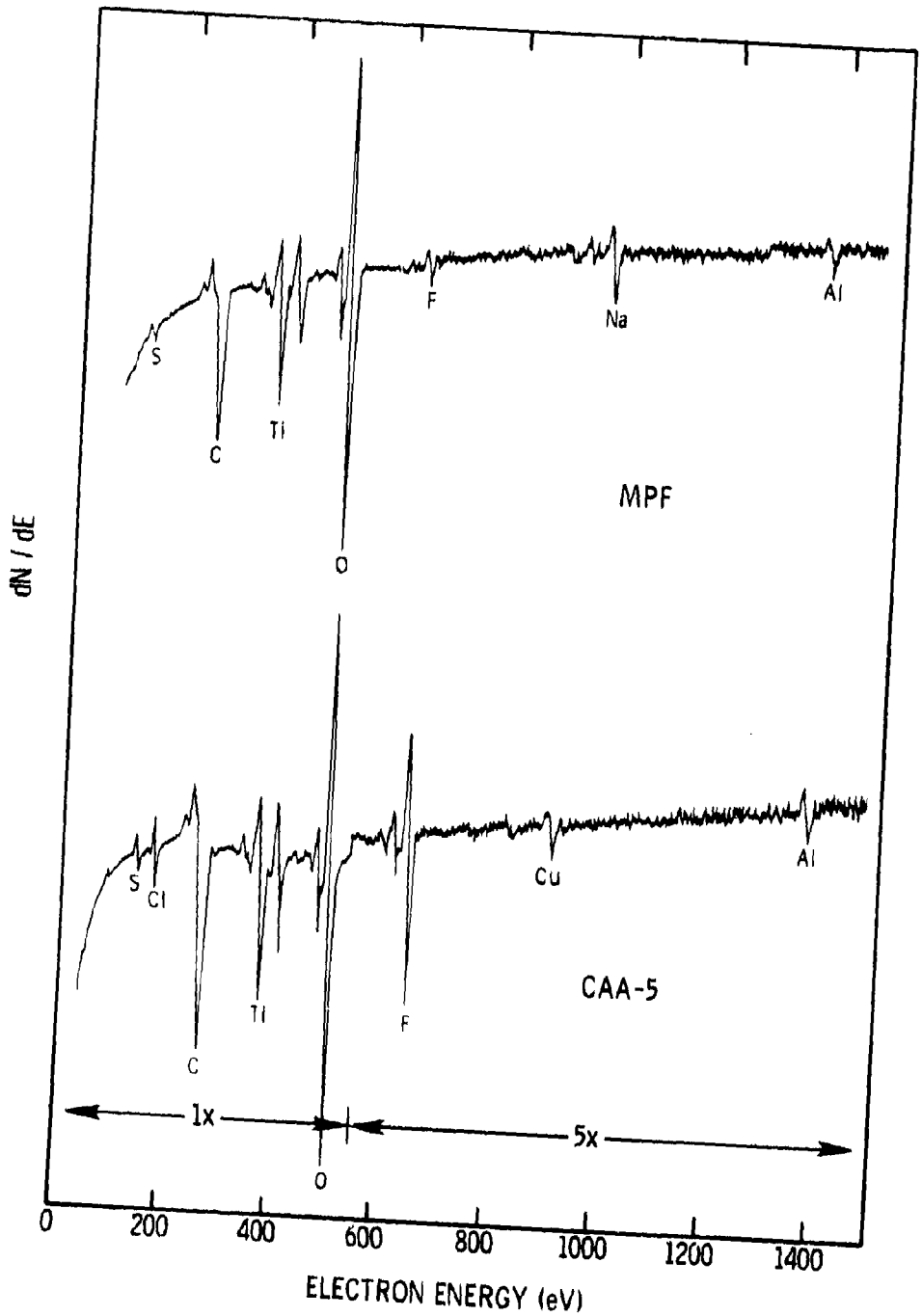

Figure 3. Auger spectra of the MPF and CAA-5 adherends showing that the kind and quantity of surface contaminants depend on the pretreatment process. Adherends prepared by the CAA process adsorb the most F of all those examined; about 6% of the surface is covered with F.

Group II Pretreatments -- The four pretreatments listed under the Group II classification all produce a large degree of macro-roughness. Imaged at low magnifications, the adherends prepared by the DA, TU, and LP treatments appear very similar. Low-magnification micrographs of the DA and TU adherends are presented in Figures 4 and 5a, respectively. In both cases, there are protrusions that extend several microns above the surface. However, these features are characteristic of the Ti substrate and not the oxide, which ranges in thickness from about 60-200 Å depending on the pretreating process. One obvious difference between the surfaces in the two micrographs is the presence of Fe, or Fe-containing particles, on the TU adherend. The origin of these micron-sized particles is unknown.

At higher magnification, other differences between these three surfaces emerge. While the DA adherend has no distinguishable fine structure, the thicker TU and LP surfaces do, as shown in Figures 5b and 6, respectively. Though both the macro- and micro-roughness of these adherends should yield some mechanical interlocking, we do not expect as large a mechanical bond component from them as from the microporous FPL or PAA oxides on Al. We suspect that the DA-treated surface will provide the least mechanical interlocking because it displays only macro-roughness. However, the TU- and LP-treated adherends should have similar and higher levels of mechanical interlocking because of their comparable macro- and micro-morphologies.

The DP surface, shown in Figure 7, is quite different from the other surfaces in this group. Apparently, dry abrasion of the Ti surface results in a heavily deformed and fragmented surface with a great deal of macroscopic roughness. This treatment also spreads Al_2O_3 over the surface. The

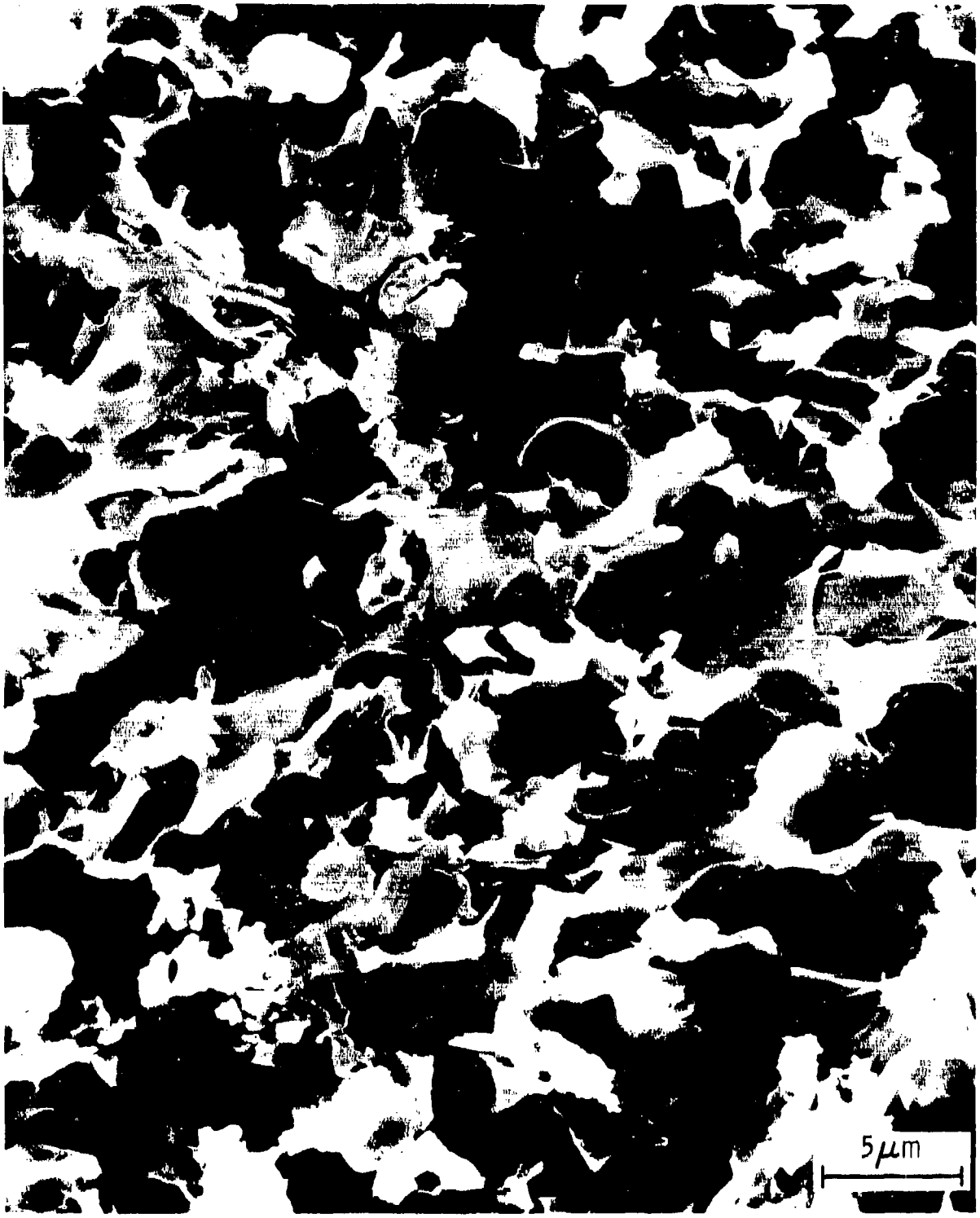

Figure 4. A collage of electron micrographs of the surface of DA-treated Ti. This adherend shows little micro-roughness but a significant degree of macro-roughness.

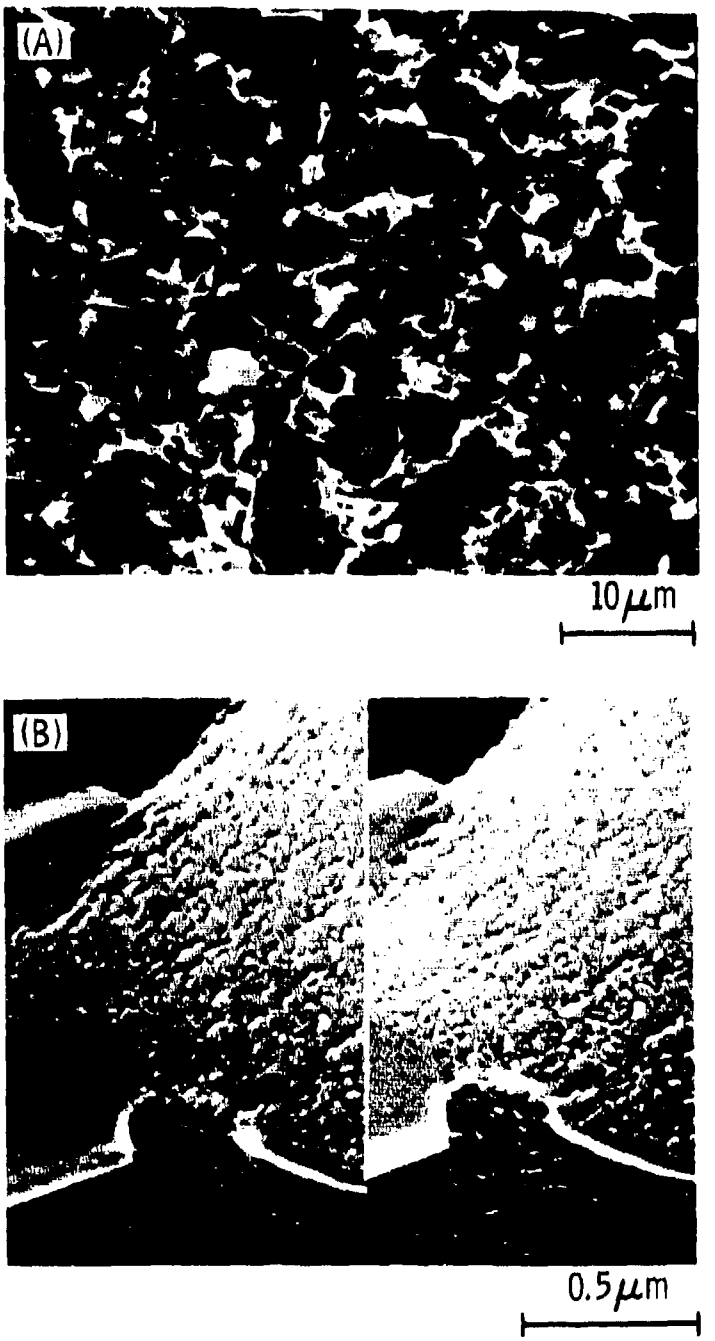

Figure 5. (A) low magnification and (B) high magnification stereo micrographs of a Turco 5578 adherend, showing both macro- and micro-roughness.

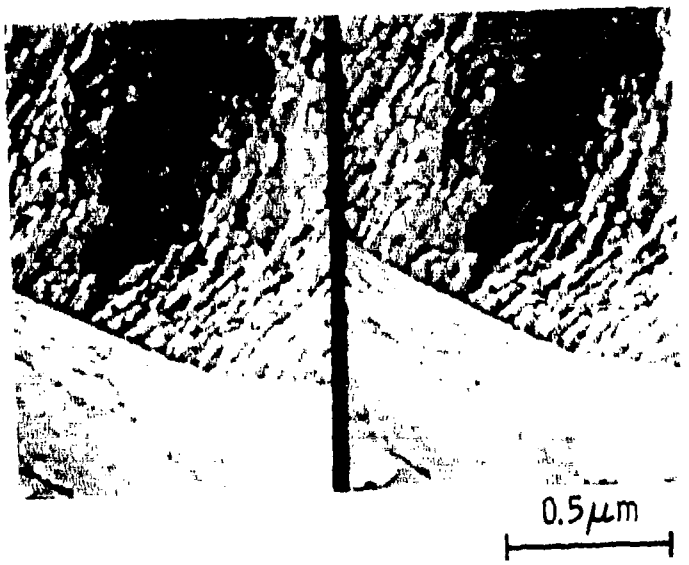

Figure 6. Stereo electron micrograph showing the micro-roughness characteristic of the LP adherend.

Figure 7. Stereo electron micrograph of the adherend formed by the dry hone PASA JELL 107 treatment.

oxide resulting from this treatment is roughly 100-200 Å thick, the large uncertainty due in part to the roughness of the surface and the presence of embedded Al_2O_3.

Auger/ESCA chemical analysis of these surfaces showed a variety of contaminants. For example, the DA (a chromate conversion coating) and PASA JELL treatments both left Cr on the surface. The PASA JELL treatments also contaminated the surfaces with fluoride. In addition, large quantities of Al were found on the adherends treated by LP and DP processes, and Fe, as discussed above, was found on the TU adherend. The effect of these contaminants on the bondability of Ti adherends will be discussed in "Failure Analysis of Wedge Test Panels."

Of the Group II adherends, only the TU oxide was examined using electron diffraction. The honing procedure could not be performed on thin foils, and the chemicals needed for the DA treatment have yet to be obtained. The TU-treated oxide yielded a ring diffraction pattern, indicating clearly that the oxide was crystalline, rather than amorphous as are those grown on Al. Nevertheless, the pattern obtained could not be indexed as rutile, anatase, or any of the standard titania structures found in the ASTM X-ray diffraction file.

Group III Pretreatments -- The adherends in this category (which include those treated by both 5V and 10V CAA and AP processes) are characterized by thick, porous oxides. At low magnification (Figure 8), the CAA surface appears smooth. However, at high magnification (Figure 9b), a porous, FPL-like oxide is observed, with a 300-Å cell size and protrusions that extend 300 Å above the cells. Unfortunately, as shown in Figure 9a, the

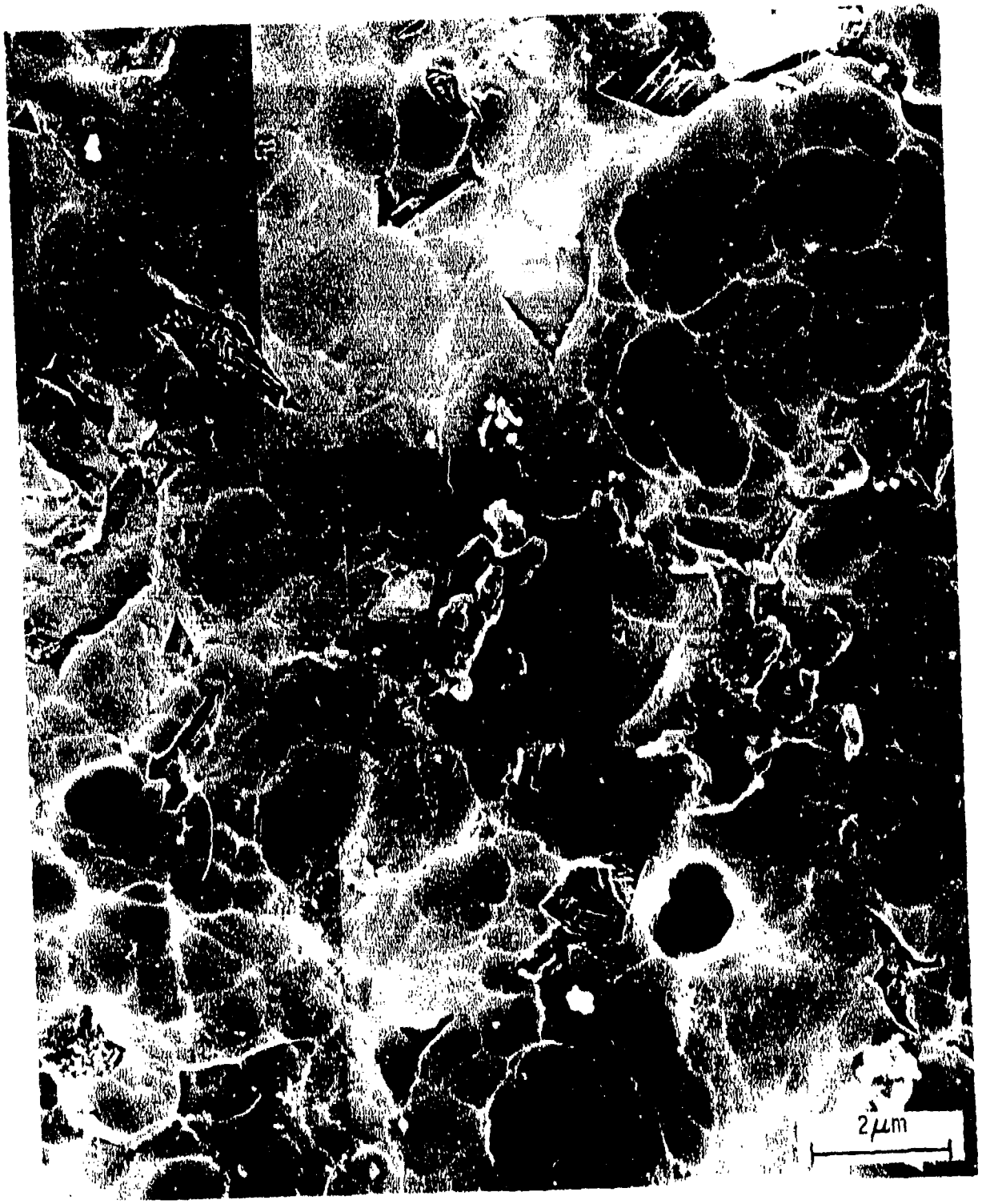

Figure 8. A collage of electron micrographs of the surface of a 5V CAA Ti adherend. This adherend exhibits little macro-roughness.

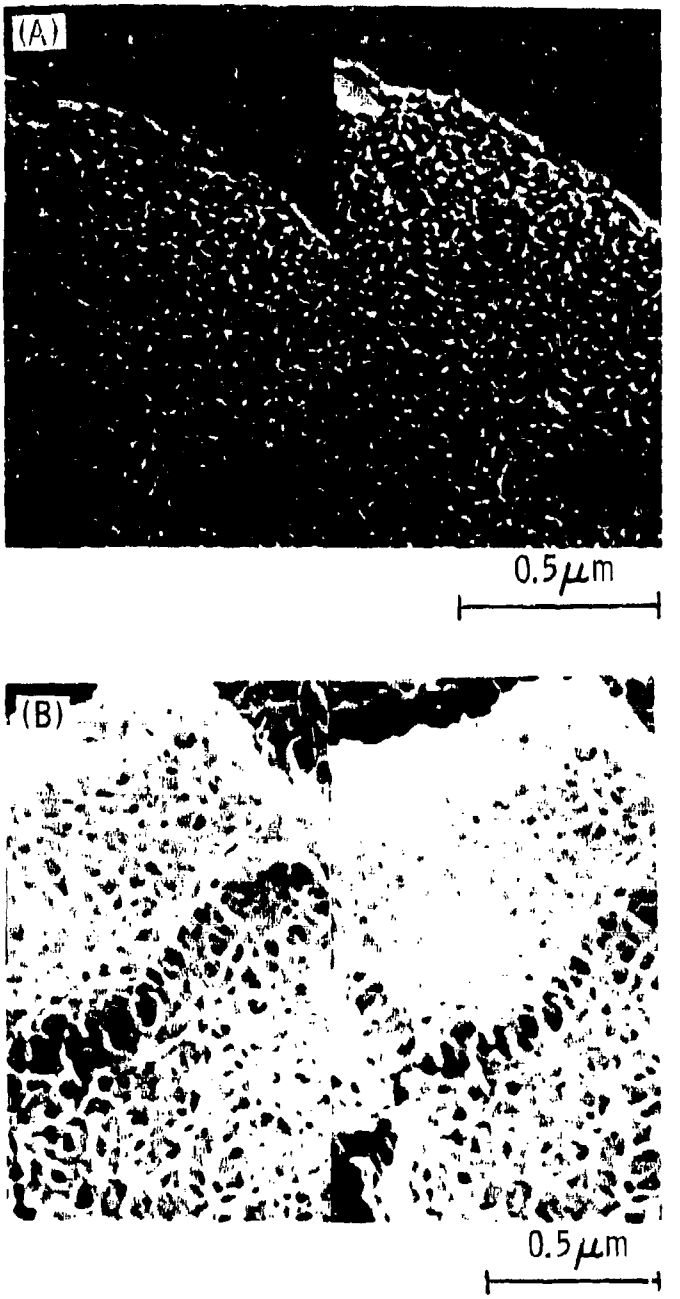

Figure 9. Stereo electron mi ographs of Ti adherends treated by (A) 5V CAA process and (B) alkaline peroxide process. Both adherends exhibit a microporous oxide that should provide a strong mechanical interlock with the primer.

porous structure does not completely cover the surface. In fact, we have observed that about 10% of the 5V CAA-treated surface is smooth, whereas a considerably greater area on the 10V CAA surface lacks microscopic roughness. The origin of the smooth areas is not known with certainty, but they are probably the result of a hydrocarbon contamination layer. Experiments at the Laboratories using combinations of chromic acid and ammonium fluoride yielded a surface with no non-porous areas.

The thicknesses of the oxides on the 5V and 10V CAA adherends were determined by Auger depth profiling to be about 400 Å and 800 Å, respectively. These oxides are considerably thicker than those for Group I and Group II adherends. For comparison, Figure 10 shows the Auger depth profile for the thin oxide on a DA Group II adherend and the thicker oxide on a 10V CAA Group III adherend. The relative thicknesses of the two may be approximately determined from Figure 10 from the ratio of the sputtering times required to reduce the O peak to half its maximum value. The ratio for these oxides is about 0.075.

Both the Auger depth profile of the CAA oxide (Figure 10) and the Auger spectra (Figure 3) indicate that about 6% of a monolayer of F is present on the surface. This amount of F, which is probably adsorbed during anodizing with the chromic acid-ammonium fluoride electrolytes, is greater than that left by any of the other treatments.

Since the alkaline peroxide adherends were processed at the Laboratories, we were able to vary their pretreatment and surface morphology considerably. Depending on bath temperature, concentration, and immersion time, the thickness and pore size of the oxide could be increased with increasing temperature. Figure 9b shows the adherend surface of Ti treated

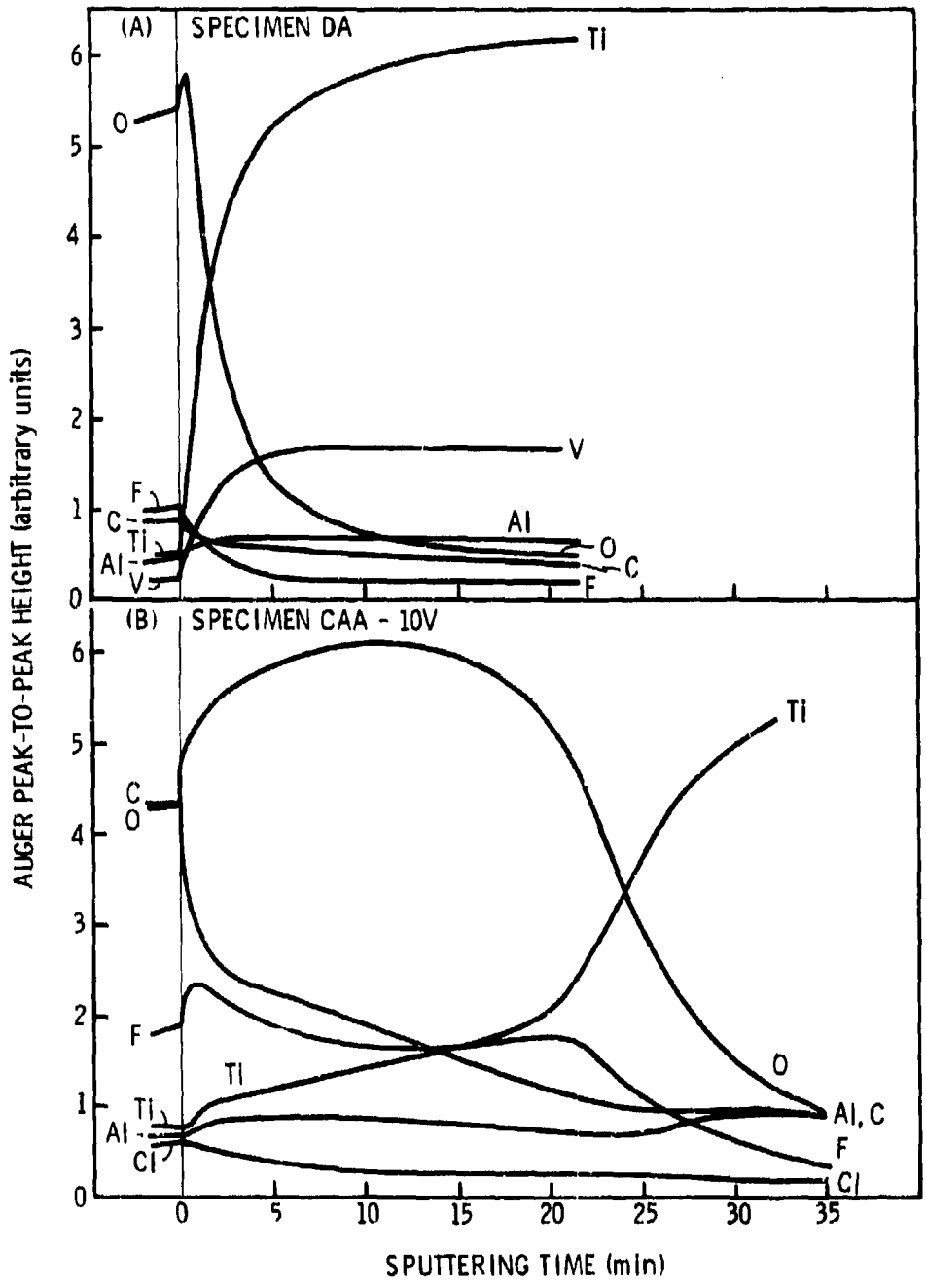

Figure 10. Auger depth profiles of (A) the thin oxide on the DA adherend and (B) the thick oxide on the 10V CAA adherend. By sputtering at 30 Å/min, the DA oxide was determined to be 60 Å thick and the CAA oxide 800 Å thick.

in 0.4M NaOH/0.5M H_2O_2 for 1 hour at 65°C. Auger depth profiling showed the oxide to be 1350 Å thick. Unlike the CAA porous oxides, these oxides had no protruding whiskers. Chemical analysis indicated that these adherends were comparatively clean, with only small quantities of Na retained on the surface.

Electron diffraction of both the CAA and AP oxides revealed a ring pattern, indicating that they were crystalline. An image of the CAA oxide, obtained using the transmission mode of the STEM, and an electron diffraction pattern of the oxide are shown in Figure 11. The diffraction pattern indicates clearly that the oxide is rutile, the tetragonal form of TiO_2. The pattern of the oxide shown in Figure 9b could not be indexed as rutile, anatase, or any other phase, using the standard diffraction file. A similar observation was made previously by Mahoon and Cotter.[9]

Stability of Ti Oxides in Humid Environments

Recent work at Martin Marietta has shown that the integrity of bonds with Al is degraded in humid environments by the transformation of FPL or PAA oxides to a pseudo-boehmite hydroxide with a "cornflake" morphology. Accordingly, we decided to determine if Ti oxides were subject to a similar transformation-induced failure. Hence, we conducted a variety of experiments to determine the stability of the oxides grown on Ti in humid environments. Specimens pretreated by all the processes listed in Table 1 were placed in a 140°F, 100% R.H. environment for 10 days and were then examined in the STEM. Additional specimens were placed in 80°C water for periods up to 18 hours. In all cases, little or no significant changes were observed, indicating that Ti oxides are much more stable than Al oxides in these environments. Figure 12 compares the stability of CAA-treated Ti

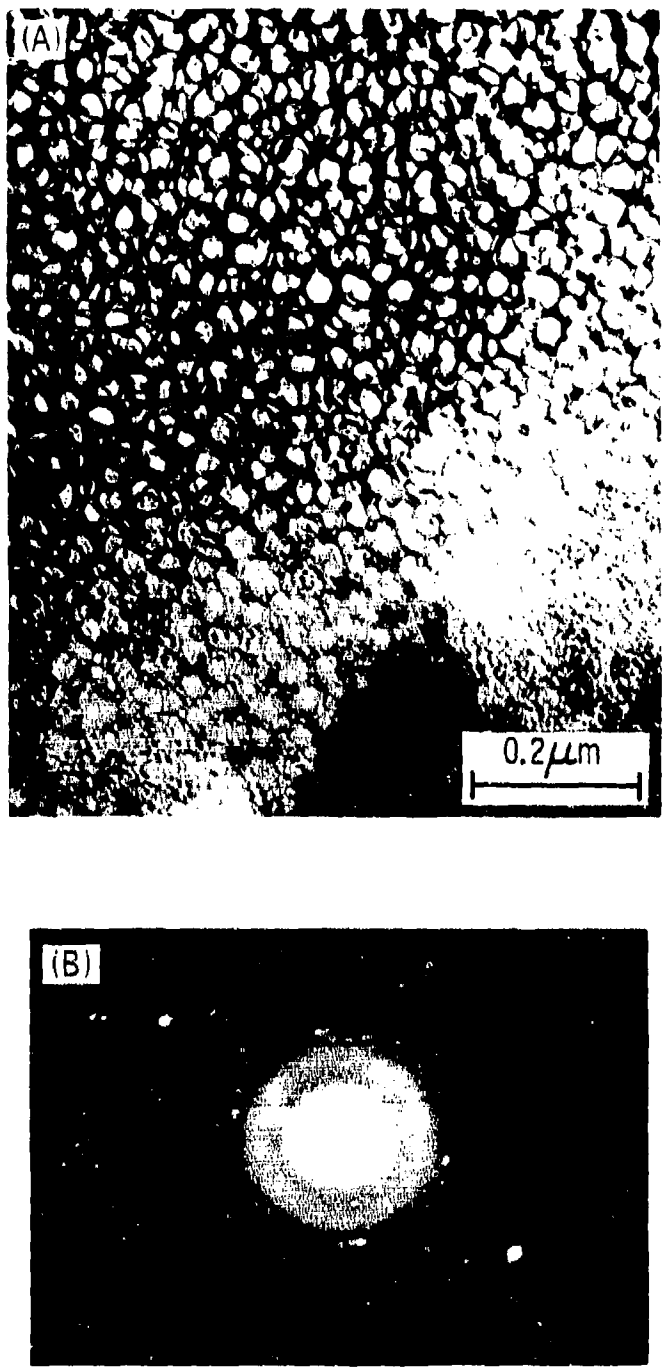

Figure 11. (A) bright field transmission electron micrograph and (B) electron diffraction pattern of an oxide grown using the 10V CAA process. The diffraction pattern identifies the oxide as having a rutile crystal structure.

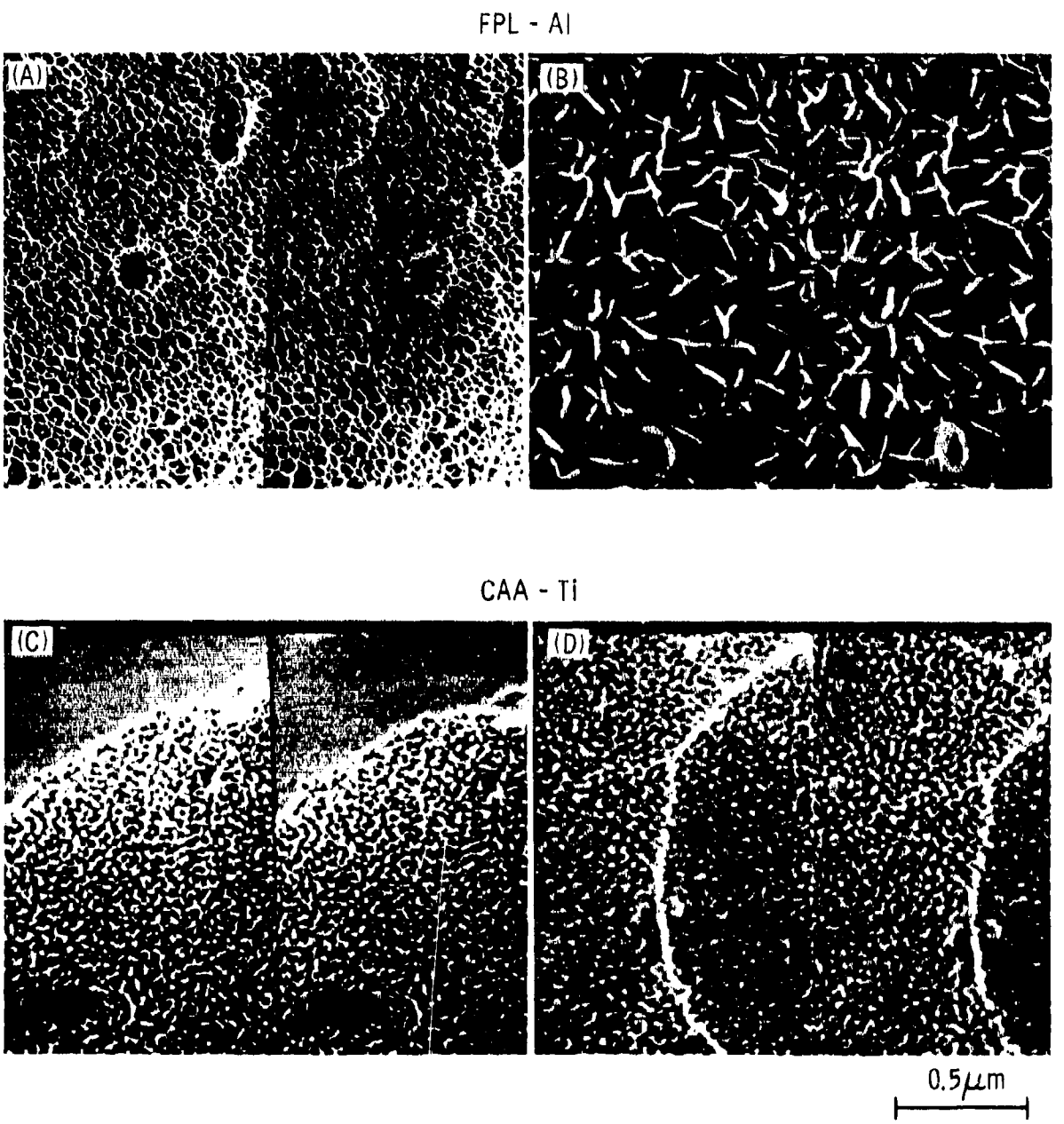

Figure 12. FPL Al and CAA Ti oxides before and after 1 hr in 80°C water. The FPL oxide on Al in (A) transforms to the "cornflake" hydroxide shown in (B) while the CAA Ti oxide in (C) shows no change (D).

and FPL-treated Al. After 2 minutes in 80°C water, the characteristic FPL morphology has been completely modified due to the transformation of the oxide to a hydroxide. On the other hand, the CAA oxide has undergone no morphological change even after being exposed for 1 hour to the hot water environment. Tests on other Ti adherends indicated that they all exhibit similar stability in these environments. Therefore, unlike Al, bonds to Ti will likely not be limited by the instability of its oxide.

Failure Analysis of Wedge Test Panels

Introduction -- The durability of bonds to Ti in a humid environment has been determined by Brown, who performed wedge tests on panels treated according to the pretreatment processes listed in Table 1 (except for AP). The panels were bonded with the FM300K/BR127 adherend/primer system. His results, plotted as crack extension vs time in a 140°F, 100% R.H. environment, are shown in Figure 13.

The results indicate that, in general, bonds to Group III adherends are more durable than those to Group II adherends, which, in turn, are more durable than those to Group I adherends. Hence, a direct correlation exists between morphology and durability for Ti adherends. For the LP- and CAA-treated adherends, the failure was obviously cohesive. In the other cases, failure appeared (with the unaided eye) to be adhesive. The results of examinations of the adhesive and metal sides of the failure surface using STEM and Auger/ESCA techniques are presented in the following sections.

Failure Analysis of Group I Wedge Test Panels -- The chemistry and morphology of the PF- and MPF-treated adherends after wedge testing, as well as the

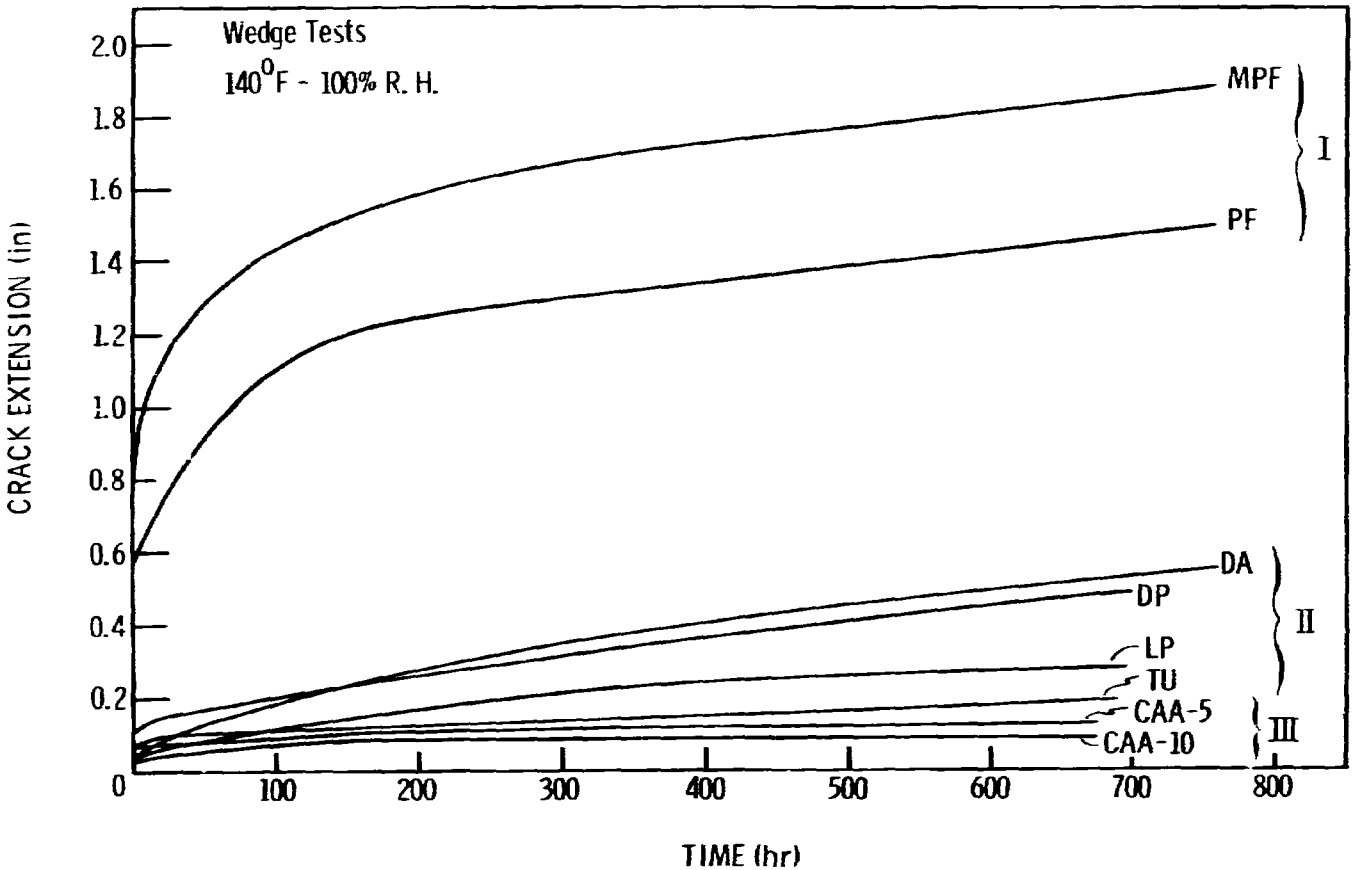

Figure 13. Results of wedge tests, performed by Brown, suggesting that adherends with high surface roughness and the ability to mechanically interlock with the adhesive provide the most durable bonds. Definitions of Groups I, II, and III can be found in the text.

primer surfaces that were in contact with these adherends, were very similar. In both cases, the primer surfaces were almost perfect negative images of the adherends to which they were bonded. Figure 14 shows a collage of photographs of the primer that debonded from the PF-1 adherend. Most of the surface displays boundary-like regions which were clearly bonded to the boundary-like depressions characteristic of phosphate fluoride adherends (see Figure 1). In addition, there are large pits on the surface that have no direct analog on the original MPF surface. These areas of the primer have undergone some cracking due to tensile stresses imposed during the wedge test.

ESCA spectra of primer that debonded from the PF adherend (Figure 15) indicate that no Ti is present on the primer after the debonding of a Group I adherend. In addition, an Auger depth profile indicated that this oxide thickness was identical with that found for the prebonded adherend.

Taken together, these results indicate strongly that the bond strength for Group I adherends is dominated by the chemical bonding component (not the mechanical bonding component). Bonds of this type, which fall into the general classification of van der Waals, or dispersion forces, are weakened in the presence of water. Hence, in a wedge test, the primer simply lifts off the Ti adherend, with relatively little energy absorption.

Failure Analysis of Group II Wedge Test Panels -- In this group, the degree of adhesive failure varied considerably with the particular adherend. Only the DP- and DA-treated adherends exhibited extensive adhesive failures. The TU adherend showed some spots of adhesive failure while the LP adherend produced none. Thus, the primer and metal surface of all but the LP surfaces were examined.

Figure 14. A collage of electron micrographs of the surface of primer that had debonded from the MPF surface after an adhesive failure. The surface is a nearly perfect negative image of the MPF adherend.

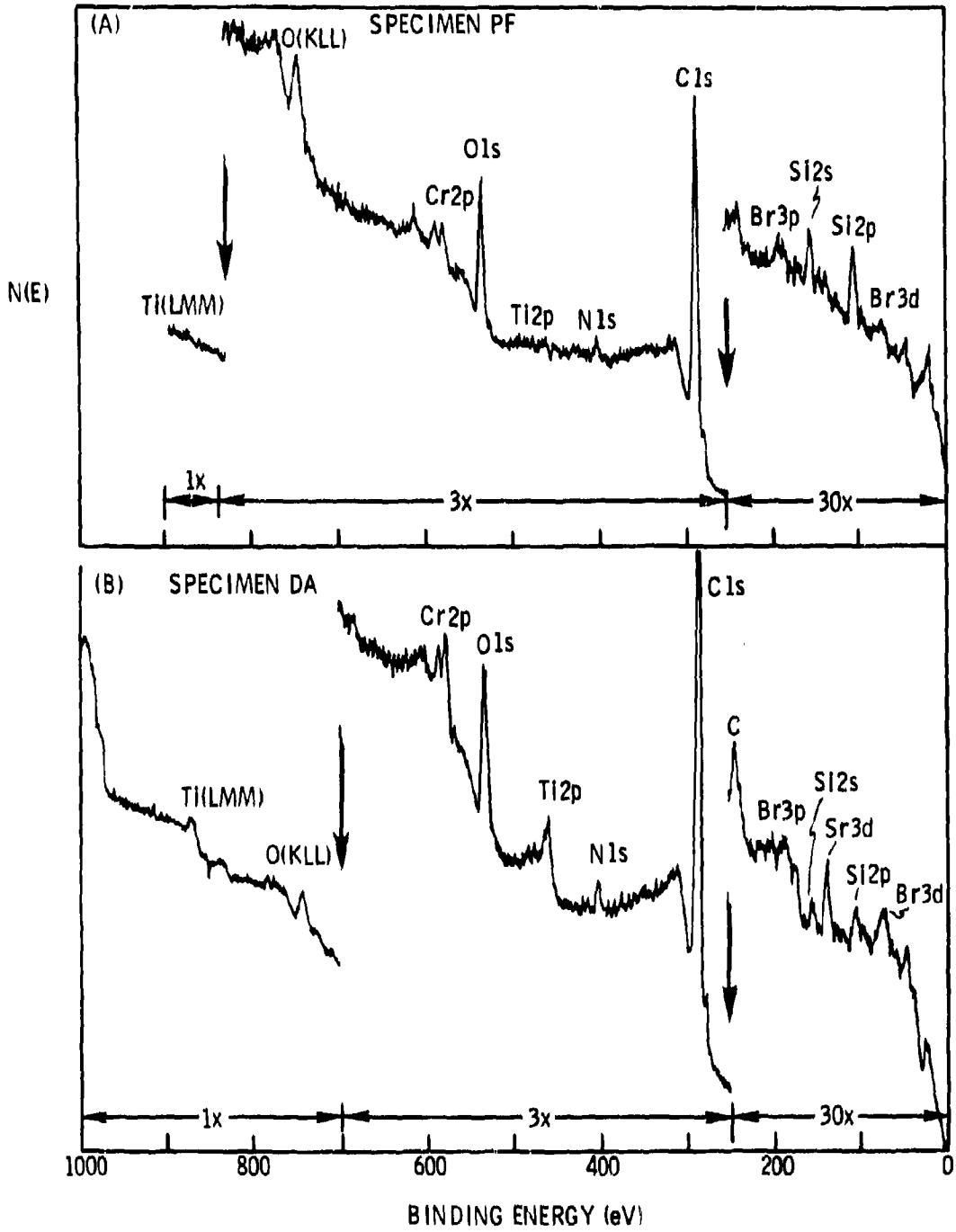

Figure 15. ESCA spectra of the BR127 primer after an adhesive failure. (A) primer bonded to the PF adherend, (B) primer bonded to the DA adherend. The spectra for (A) show no Ti, while those for (B) do show Ti, indicating that the DA adherend provides some mechanical interlocking with the primer.

The primer and Ti portions from the failed DA panels, shown in Figures 16 and 17, indicate that the failure mechanism for debonding in a Group II adherend is different than for a Group I adherend. In this case, the surface morphology of the primer is not a simple negative image of the prebonded surface (shown in Figure 4). Although the primer surface does show the macro-roughness characteristic of the DA-5 surface, the depressions in the primer are less regularly distributed and appear more fragmented. The Ti side of the DA wedge test panel also appears much more irregular than the prebonded surface (Figure 4). Apparently, separation of the primer and Ti surface caused some fracture of the Ti protrusions (as well as deformation of the primer). Thus, some Ti should remain on the primer surface, and, indeed, the ESCA spectra of the primer surface, shown in Figure 15, reveal a Ti peak. For comparison, the ESCA spectra of the primer bonded to a Group I adherend, Figure 15, show no Ti peak. Hence, the mechanical bond reinforcement for this Group II adherend produces less crack extension and adhesive failure than for a Group I adherend because crack propagation along the DA primer-metal interface is an energy absorbing process yielding a relatively high fracture toughness.

The improved performance with the TU and LP adherends was probably due to their greater micro-roughness, compared to the DA surface. Actually, since the TU and LP adherends were so similar in morphology, it was somewhat surprising to find that the TU adherend exhibited some adhesive failure (as judged by the unaided eye), while the LP adherend did not. However, when we examined the metal side of the TU failure surface with the STEM, we found a thin layer of primer covering the surface (Figure 18), i.e., the failure was actually cohesive.

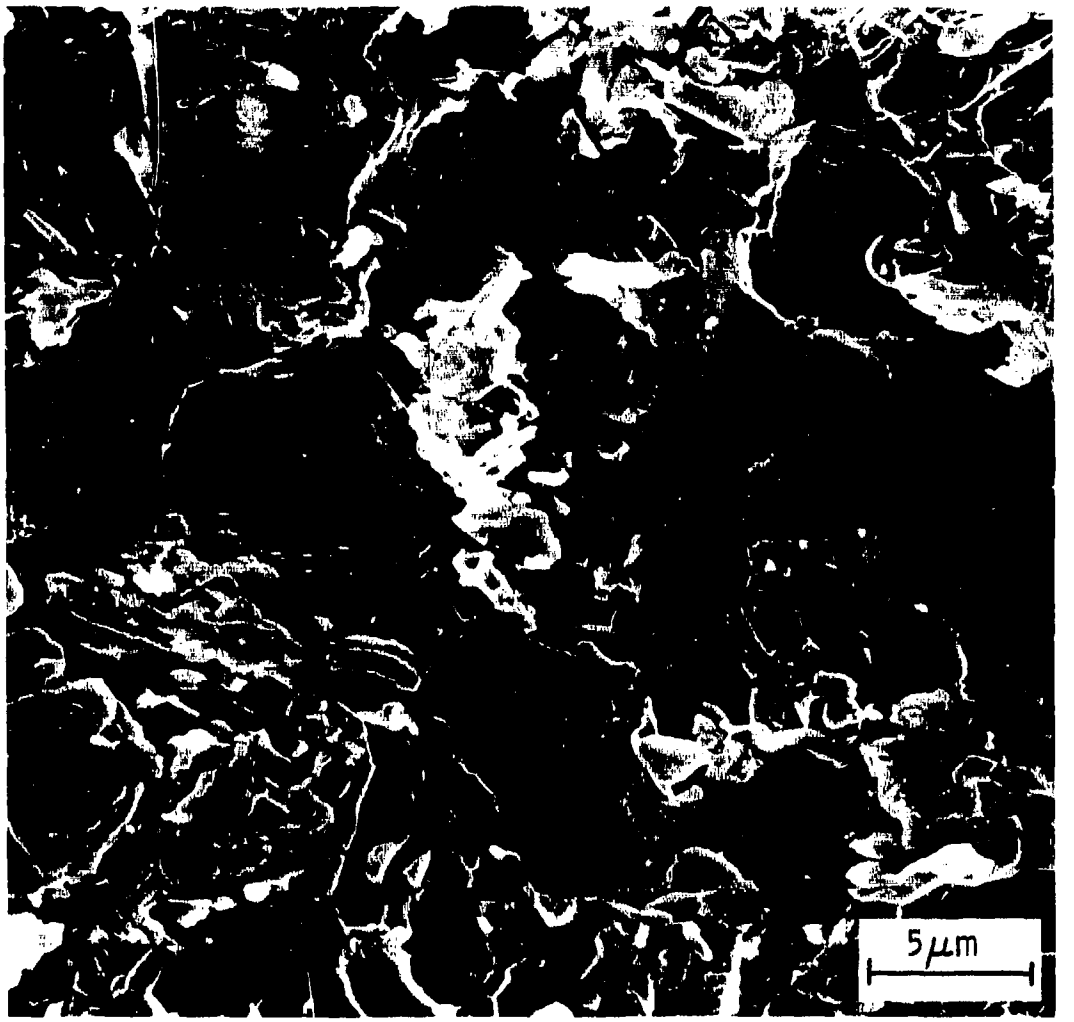

Figure 16. A collage of electron micrographs of the primer side of an adhesively failed DA-treated Ti wedge test panel.

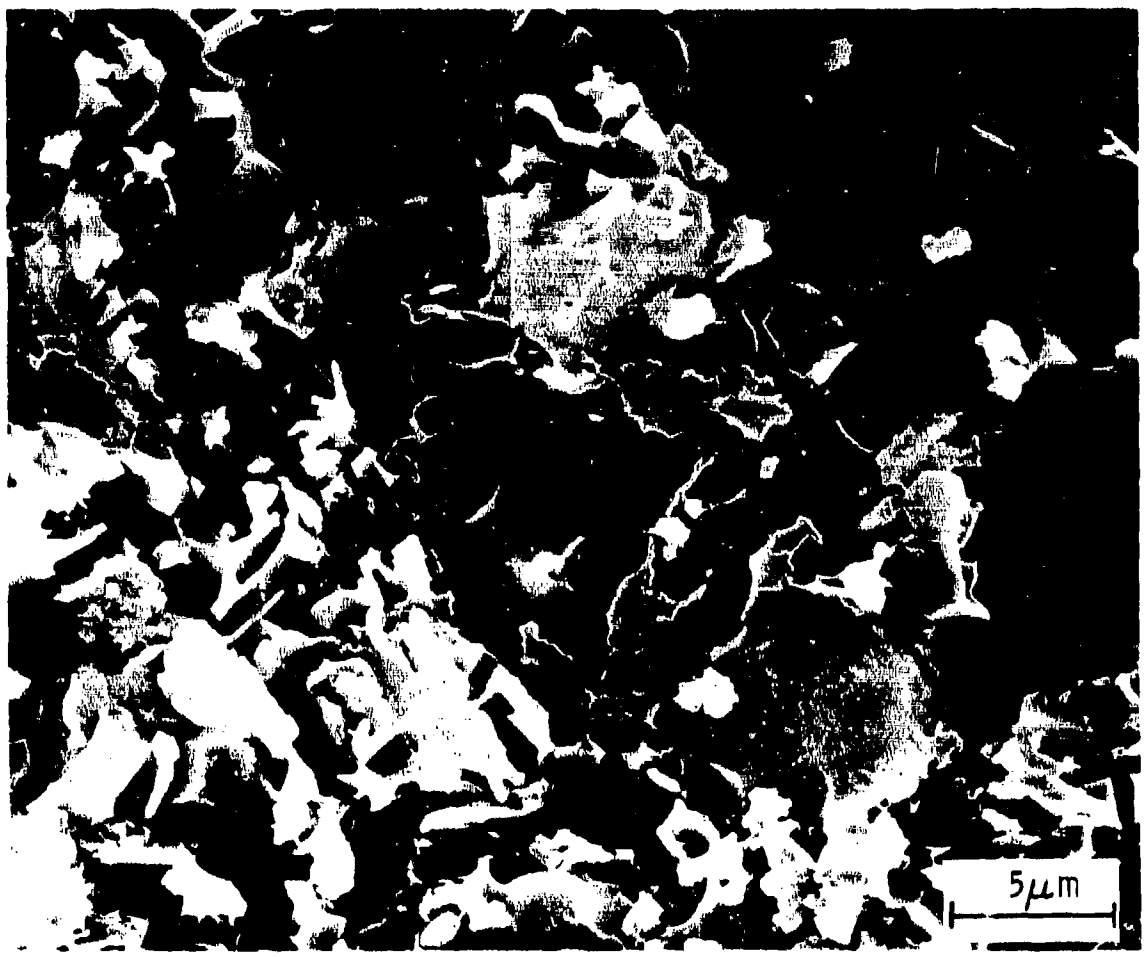

Figure 17. A collage of electron micrographs of the Ti side of an adhesively failed DA-treated Ti wedge test panel.

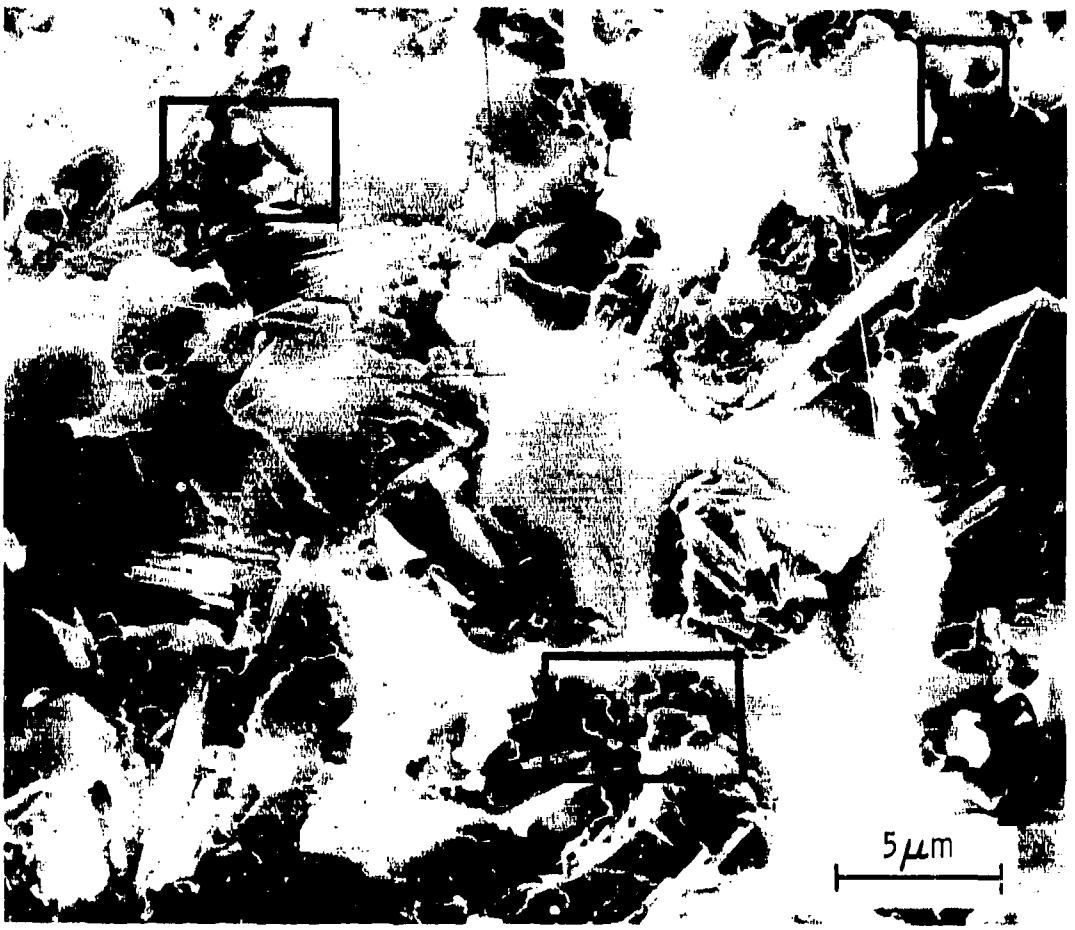

Figure 18. A collage of electron micrographs of the Ti side of a failed TU-treated Ti wedge test panel. A thin layer of primer covers the surface. The upper two boxed areas point to regions where Fe particles were found. The area within the lower rectangle was clearly bonded to a cluster of Fe particles.

It should also be noted that Fe particles were found on this surface just as on the prebonded surface. Fe particles were also found on the adhesive side of the failure (Figure 19). The presence of Fe on both sides of the failure surface suggests that failure actually occurred along the line of Fe particles. Thus, we suspect that Fe particles act as stress raisers which localize failure near the Ti adherend. This chemical difference between the TU and LP adherends appears to explain their slightly different failure modes.

The failure surfaces of the DP wedge test panels were not as revealing as the DA surfaces. Because the prebonded surface was very highly deformed, it was difficult to detect any additional deformation after bonding. ESCA of the adhesive side of the failure did not reveal any Ti, suggesting that this surface affords the least mechanical interlocking of the Group II adherends.

Failure Analysis of Group III Wedge Test Panels -- The failure of the bonds to CAA-treated adherends, the only ones tested in this group, was cohesive. Apparently, the porous adherends provided by the CAA process allow sufficient mechanical interlocking between the primer and Ti panel that the path of least resistance for crack propagation is through the adhesive, rather than along the primer-adherend interface.

Failure Analysis of Lap Shear Panels

Wegman obtained stress durability data (140°F, 100% R.H.) on Ti panels bonded with different sets of adhesive primer systems to MPF and LP adherends. The failed specimens were subsequently sent to us for analysis.

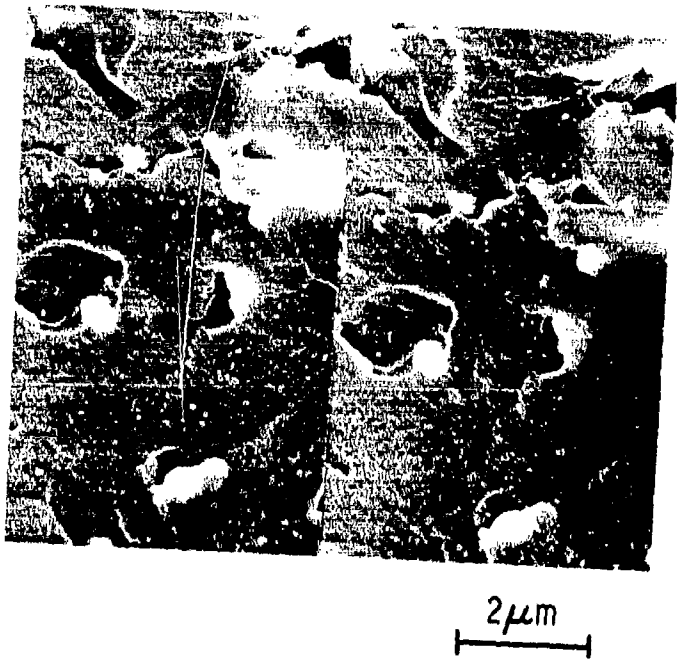

Figure 19. A stereo electron micrograph of a Fe particle embedded in the primer (on the primer side) of a failed TU wedge test panel.

The MPF lap shear specimens showed extensive adhesive failure, as did the failed MPF wedge test panels. But, unlike the LP wedge test panels, the LP failed lap shear durability panels showed adhesive failure.

The Ti side of the MPF failed lap shear specimen showed some unusual markings. Figure 20 shows a stereo micrograph of a part of the adhesively failed surface of this specimen, which had been bonded using the EA9628H/BR127 adhesive/primer system. The specimen pulled apart after loading for 61.2 hours with 800 psi. The surface shown does not display any of the ridges observed previously but does exhibit a fine structure that has not yet been clearly identified (areas that show these markings are too small to be chemically analyzed using Auger/ESCA techniques). Thus, it appears that pure water does not cause changes in the oxide, but other environments, such as salt water, may.

Adhesively failed LP lap shear panels were also examined. These specimens proved much more durable than MPF panels (2000 psi for 1372 hours before debonding) and showed no evidence of morphological degradation: the macro- and micro-structure observed on the surfaces were similar to those found on prebonded coupons.

To date, the results on the lap shear panels are incomplete and it is not yet possible to draw specific conclusions from them. However, both the mechanical data and the failure analysis agree reasonably well with wedge test results.

The Effects of Pretreatment Variables on the Adherends

During the course of this work, we have experimented with new pretreatment procedures, as well as standard ones. Some of our observations are summarized below.

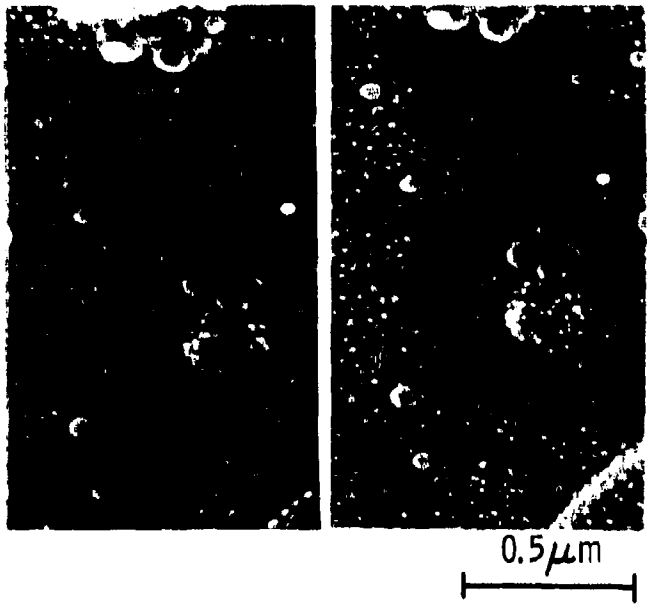

Figure 20. Stereo electron micrograph of the surface of a MPF lap shear specimen which had failed adhesively when loaded for 61.2 hr at 800 psi in a 140°F, 100% R.H. environment.

1) The immersion time of Ti in a phosphate fluoride process affects the size of boundary-like regions on the surface, i.e., the longer the immersion bath, the larger the cells.

2) An adherend morphology similar to that observed for the 10V CAA-treated specimens supplied to us can be developed with the following electrolyte and conditions:

   5 wt.% chromic acid

   1 g/liter NH_4F

   10V

   Anodized for 20 min at room temperature.

   Substituting phosphoric acid for the chromic acid in this process does not yield a porous oxide.

3) Anodizing (5-20V) in phosphoric acid, chromic acid, sodium hydroxide, or oxalic acid (without any NH_4F) does not yield a porous oxide.

4) Hot temperature rinses (65°C) are required after a phosphate fluoride treatment to remove excess KF and Na_3PO_4 contaminants.

5) Depending on concentration, treatment temperature, and time, the pore size resulting from an alkaline peroxide treatment can be varied from over 1000 Å to under 100 Å. Large pores result under conditions of high temperature, long treatment times, and low concentrations of NaOH.

4. DISCUSSION

The results of this study emphasize the importance of bonding to an adherend that is both environmentally stable and sufficiently rough to provide a mechanical interlock with the adhesive. Bonds made to suitable adherends are both strong and durable.

Our studies of the stability of Ti adherends in the range of temperatures and humidity used for wedge and lap shear durability testing indicate that: 1) the oxide undergoes no significant morphological changes, and 2) no dramatic oxide-to-hydroxide transformation takes place, as for Al. Previous workers have suggested that oxides grown on titanium undergo a transformation which converts the unstable form of TiO_2 (such as anatase or brookite) to the stable rutile form, resulting in reduced durability. Studies by Hamilton[13] have suggested that the anatase form of TiO_2 is most favorable for bonding since it has a lower affinity for water than does the rutile form. Hence, the transformation from anatase to rutile weakens the bond and reduces durability. We have not completed studies of structural changes of the various oxide adherends with time, but our study of the as-grown oxides seems to refute this explanation for differences in durability. We have not observed the anatase form of the oxide on any of the adherends. In addition, and in direct contradiction to Hamilton, the oxide on the CAA adherend, which is in the rutile form, shows the greatest durability. Hence, it is unlikely that any crystal structure transformation can account for relative differences in bond durability.

---

13. W.C. Hamilton and G.A. Lyerly, Gillette Research Institute, Technical Report 4105, 1971.

Rather, the chemical and morphological stability of the treated Ti adherends is the key to understanding their relative durability. For bonds to stable oxides, bond durability is related to initial bond strength. Hence, we find that the greater the mechanical interlocking of the adherend with the epoxy, the greater the bond durability. This explanation accounts for the dramatic difference in bond durability between PF and CAA adherends. While the smooth PF adherend produces a large adhesive crack extension, the micro-rough CAA adherend does not permit any fracture at the oxide/primer interface.

In contrast, it should be noted that the FPL oxide on Al, although micro-rough, allows adhesive crack propagation due to the instability of the oxide in moist environments. Thus, even though a micro-rough oxide ensures good initial bond strength for Al, it does not by itself provide adequate long-term durability. However, the combination of oxide stability and micro-roughness that can be developed on Ti by the CAA or alkaline peroxide processes indicates that the future of Ti adhesively bonded structures is very bright.

5. CONCLUSIONS

The important conclusions of this study on the bondability of Ti adherends are:

(1) The PF and MPF processes produce thin oxides with little micro- or macro-roughness and low bond durability.

(2) The DA, DP, CP, and TU processes yield thin, macro-rough oxides that produce intermediate to high bond durability, depending on the degree of micro-roughness.

(3) The CAA process yields a thick, porous, FPL-like oxide that induces high bond durability.

(4) Only the CAA oxide was observed to possess the rutile form of titanium.

(5) The treated Ti surfaces are much more stable in hot, humid environments than those on Al.

(6) Analysis of wedge test adhesive failures of the PF and MPF adherends suggests that the primer simply lifts off the Ti adherend, with relatively little energy absorption.

(7) Analysis of wedge test adhesive failures of the DA adherend suggests that crack extension requires deformation of the adherend surface to pull the primer and adherend apart.

(8) Analysis of wedge test samples using CAA adherends indicates that the failure is always cohesive.

REFERENCES

1. P.F.A. Bijlmer, J. Adhesion 5, 319 (1975).

2. P.F.A. Bijlmer and R.J. Schliekelman, SAMPE Quarterly 5(1), 13 (1973).

3. A. Pattnaik and J.D. Meakin, Franklin Institute Research Laboratories Technical Report 4699, 1974.

4. T. Smith, Rockwell International Report AFML-TR-74-73, 1975.

5. J.M. Chen, T.S. Sun, J.D. Venables, and R. Hopping, Proc. 22nd National SAMPE Symposium (San Diego, CA, 1977) p. 25.

6. J.D. Venables, D.K. McNamara, J.M. Chen, T.S. Sun, and R.L. Hopping, Appl. Surface Sci. 3, 88 (1979).

7. R.F. Wegman and M.J. Bondnar, SAMPE Quarterly 5, 28 (1973).

8. M.J. Felsen, "Materials Synergisms," Proc. 10th National SAMPE Technical Conference Series, Vol. 10, p. 100, 1978.

9. A. Mahoon and J. Cotter, ibid., p. 425.

10. Y. Maji and J.A. Marceau, U.S. Patent 3,959,091, May 25, 1976.

11. T.S. Sun, D.K. McNamara, J.S. Ahearn, B.M. Ditchek, J.D. Venables, and J.M. Chen, submitted to Applications of Surface Science.

12. K.W. Allen and H.S. Alsalim, J. Adhesion 6, 229 (1974).

13. W.C. Hamilton and G.A. Lyerly, Gillette Research Institute, Technical Report 4185, 1971.

DISTRIBUTION LIST

BONDABILITY OF TI ADHERENDS

Commander
Naval Air Development Center
Warminster, PA 18974

Attn: S. R. Brown
Code 60622

Commander
U.S. Army ARRADCOM
Dover, NJ 07801

Attn: R. Wegman
DRDAR-LCA-OA

Air Force Materials Laboratory
Air Force Wright Aeronautical Laboratories
Wright-Patterson Air Force Base
Ohio 45433

Attn: H. S. Schwartz, AFML/MBC
W. Baun, AFML/MBM

National Aeronautics & Space Administration
Langley Research Center
Hampton, VA 23665

Attn: J. B. Nelson
NASA-LRC-MD

Advanced Structures Division
801 Royal Oaks Drive
Monrovia, CA 91016

Attn: G. L. Maxwell

Bell Helicopter Textron
P. O. Box 482
Fort Worth TX 76101

Attn: N. L. Rogers
Chemical and Process Lab

Boeing Aerospace Company
P. O. Box 3999
Seattle, WA 98124

Attn: S. G. Hill, MS 47-01
D. B. Arnold, MS 41-37

Grumman Aerospace Corp.
Bethpage, L.I., N.Y. 11714

Attn: W. Horney
S. Westerback
A04/12

Lockheed-California Company
P. O. Box 551
Burbank, CA 91520

Attn: E. L. Riggs
Dept. 76-31

McDonnell Douglas Corp.
Box 516
St. Louis, MO 63166

Attn: T. C. Grimm
Dept. 347, Bldg. 32

Rockwell International
Military Aircraft Division
4300 East Fifth Street
Columbus, OH 43212

Attn: J. G. Fasold
Dept. 071, Group 522

Rohr Industries, Inc.
8200 Arlington Ave.
Riverside, CA 92503

Attn: W. D. Brown
Group Engineer

Sikorsky Aircraft
North Main Street
Stratford, CT 06652

Attn: H. Butts, Composite Blade Mfg. and Dev.
G. Cheetam, Structures and Materials

Vought Advanced Technology Center
P. O. Box 226144
Dallas, TX 74266

Attn: J. A. Hoffner
Unit R-92000

American Cyanamid Company
Bloomingdale Plant
Old Post Road
Havre de Grace, MD 21078

Attn: R. Politi
Manager, R and D

Hysol Division
The Dexter Corporation
2850 Willow Pass Road
Pittsburg, CA 94565

Attn: J. Bagwell

Narmco Materials, Inc.
600 Victoria St.
Costa Mesa, CA 92627

Attn: D. Black
Technical Service Mgr.

National Aeronautics and Space Administration
Headquarters
Washington, D.C. 20546

Attn: C. Bersch
Code RTM6

Naval Air Systems Command
Washington, D.C. 20361

Attn: R. Schmidt, Code AIR-320A
S. Saletros, Code AIR-5163C2 (25 copies)